Article:
Yazdaninejad, M, Amjady, N and Dehghan, S orcid.org/0000-0001-9619-6471 (2020) VPP Self-Scheduling Strategy Using Multi-Horizon IGDT, Enhanced Normalized Normal Constraint, and Bi-Directional Decision-Making Approach. IEEE Transactions on Smart Grid, 11 (4). pp. 3632-3645. ISSN 1949-3053

https://doi.org/10.1109/tsg.2019.2962968

VPP Self-Scheduling Strategy Using Multi-Horizon IGDT, Enhanced Normalized Normal Constraint, and Bi-Directional Decision-Making Approach

Mohsen Yazdaninejad, Nima Amjady, *Senior Member*, *IEEE*, and Shahab Dehghan, *Senior Member*, *IEEE*

***Abstract*—This paper presents a new robust self-scheduling strategy for virtual power plants (VPPs) considering the uncertainty sources of electricity prices, wind generations, and loads. Multi-horizon information-gap decision theory (MH-IGDT) as a non-deterministic and non-probabilistic uncertainty modeling framework is proposed here to specifically model the uncertainty sources considering their various uncertainty horizons. Since each uncertain parameter tends to optimize its uncertainty horizon competitively for a particular value of the uncertainty budget, the proposed MH-IGDT model is formulated as a multi-objective optimization problem. To solve this multi-objective problem, enhanced normalized normal constraint (ENNC) method is presented, which can obtain efficient uniformly-distributed Pareto optimal solutions. The proposed ENNC includes augmented normalized normal constraint method and lexicographic optimization technique to enhance the search performance in the objective space. To address the unsolved issue of being risk-averse or risk-seeker for a VPP in the market, a bi-directional decision-making approach is presented. This decision maker comprises an ex-ante performance evaluation method and a forward-backward dynamic programming approach to hourly find the best Pareto solution within the generated risk-averse and risk-seeker Pareto frontiers. Simulation results of the proposed self-scheduling strategy are presented for a VPP including dispatchable/non-dispatchable units, storages, and loads.**

***Index Terms*—Bi-directional decision making, ENNC, Lexicographic optimization, MH-IGDT, VPP self-scheduling strategy.**

NOMENCLATURE

A. Functions

$\mathcal{F}(.)$	Profit of VPP coalition ($).
$C_u(.)$	Operation cost of unit u ($).
$\pounds(.)$	Feasible part of solution space.

B. Indices and Sets

b	Index of contractual buses (buses through which VPP members are connected to the grid).
j	Index of Pareto optimal solutions.
k, k'	Index of states in FBDP.
l	Index of loads.
t, t'	Index of time of scheduling horizon.
u	Index of dispatchable (D)/wind (W)/storage (S) units of VPP coalition, i.e., $u \in \{D, W, S\}$.
ϑ	Index of uncertain LMP (λ)/wind generation (w)/ load (l), i.e., $\vartheta \in \{\lambda, w, l\}$.
ζ	Index of performance evaluation scenarios.
$\mathcal{R}_\vartheta$	Envelope-bound region for uncertain parameter ϑ.
$\Omega_D/\Omega_S/\Omega_W$	Set of dispatchable/storage/wind units of VPP.
$\Omega_{l^b}/\Omega_{S^b}$	Set of VPP loads/storages connected to bus b.
$\Omega_{D^b}/\Omega_{W^b}$	Set of VPP dispatchable/wind units connected to bus b.
Ω_{u^b}	$\Omega_{u^b} = \Omega_{D^b} \cup \Omega_{W^b} \cup \Omega_{S^b}$

C. Parameters

A_u	No-load cost of unit u ($).
B_u	Fuel-cost of unit u ($/MWh).
M	A sufficiently large number.
P_{lt}	Uncertain load l at time t (MW).
RD_u/RU_u	Ramp down/up rate limit of unit u (MW/h).
SD_u^c/SU_u^c	Shutdown/startup cost of unit u ($).
SD_u^r/SU_u^r	Shutdown/startup ramp rate limit of unit u (MW/h).
UB	Uncertainty budget.
ρ_{lt}	Fixed consumption price of load l at time t ($/MWh).
λ_{bt}	LMP of bus b at time t ($/MWh).
τ_u^{on}/τ_u^{off}	Minimum up/down time limit of unit u (h).
σ_u	Self-discharging (leakage) rate of storage u.
μ_u^r/μ_u^s	Discharging/charging efficiency of storage u.

D. Variables

E_{ut}	Stored energy of storage u at time t (MWh).
I_{ut}	Binary commitment variable of unit u at time t.
I_{ut}^r/I_{ut}^s	Binary discharging/charging variable of storage u at time t.
P_{bt}^N	Injected power to the grid through bus b at time t (negative/positive values indicate purchased/sold powers from/to the grid) (MW).
P_{ut}	Produced power of unit u at time t (MW).
P_{ut}^r/P_{ut}^s	Discharging/charging power of unit u at time t (MW).
x_{ut}/y_{ut}	Binary startup/shutdown variable of unit u at time t.
z_{bt}	Auxiliary binary modeling variable to determine excess/deficit injected power of bus b to the grid at time t.
α_ϑ	Uncertainty horizon of uncertain parameter ϑ.

E. Vectors and Matrices

M. Yazdaninejad and N. Amjady are with the Department of Electrical Engineering, Semnan University, Semnan, Iran (e-mail: amjady@semnan.ac.ir).
S. Dehghan is with the School of Electronic and Electrical Engineering, University of Leeds, Leeds, UK.

Ξ Vector of decision variables.
Θ Vector of uncertain parameters.

In this paper, superscripts $\bar{}$, $\check{}$, $\hat{}$, ζ, and j indicate forecast, risk-averse, risk-seeker, performance evaluation scenario, and Pareto solution associated variables, respectively. The other parameters and variables are defined in the paper.

I. Introduction

A. Background and Motivation

INCREASING penetration of distributed energy resources (DERs), diminishing subsidy schemes, and increasing energy prices lead to the emergence of virtual power plants (VPPs) in electricity markets. VPPs, as a flexible portray of DERs, can facilitate wholesale market participation for the VPP coalition members and enhance competition in the market [1]. Having a suitable self-scheduling strategy to maximize the profit of selling aggregated generation is an essential factor for the economic stability of VPPs. However, this self-scheduling strategy encounters various uncertainty sources (such as the uncertainty of the market prices as well as the uncertainties of VPP renewable generations and load demands) which can jeopardize the economic stability of VPP and finally threaten the existence essence of the coalition. Thus, some research works have recently studied the VPP bidding strategy problem, which are briefly reviewed in the following.

In [2], a deterministic bidding strategy for VPP market participation has been proposed. However, this method ignores all uncertainty sources of the problem. Operation scheduling problem of a risk-averse VPP has been modeled by two-stage stochastic programming in [3]. In [4] and [5], the bidding strategy of VPP in joint energy and reserve markets is constructed by scenario approach and two-stage stochastic programming, respectively. Conditional value-at-risk is also adopted in [5] as a risk measure. The uncertainty of day-ahead (DA) market price and wind generation is modeled through point estimate method, and a probabilistic price-based unit commitment is used to obtain the VPP bidding strategy in [6]. A stochastic bi-level optimization model for participating VPP in DA and balancing markets has been proposed in [7]. However, scenario-based approaches may suffer from two disadvantages: 1) Requiring probability distribution functions (PDF) of uncertain parameters which may not be easy-to-obtain. 2) Requiring an adequately large number of scenarios to model behavior of uncertain parameters which can increase the problem size and computation burden [8].

Robust optimization has been used to construct the bidding strategy of a cluster of small wind power plants, energy storage facilities, and price-responsive demands in [9]. In [10], the uncertainty of DA market price and customers' demand has been addressed by robust optimization approach in the VPP self-scheduling problem through supposing a linear relation between the market prices and the customers' demand. However, robust optimization cannot optimize opportunistic self-scheduling solutions using favorable fluctuations of uncertainties, since it essentially looks for the worst-case realization of the uncertain parameters to provide the highest robustness.

B. Contributions and Assumptions

In this paper, VPP self-scheduling problem considering the uncertainty sources of electricity price as well as VPP wind generations and loads is addressed through a multi-horizon information-gap decision theory (MH-IGDT) approach. Instead of making assumption on multifold uncertain parameters and maximizing the VPP total profit, the proposed MH-IGDT model optimizes uncertainty horizons and provides short-term operation schedules of the members so that a minimum predefined admissible profit is achieved. From a VPP decision-maker point of view, defining a target value on the total profit is more sensible than holding assumption on PDF or introducing confidence interval on each uncertain parameter. However, previous applications of information-gap decision theory (IGDT) for uncertainty modeling are uni-directional frameworks. Some of these frameworks consider solely the robust side, e.g., [11], and some other ones can only select either a risk-averse or a risk-seeker strategy for all hours of the self-scheduling horizon, e.g., [12]. In addition, the uni-directional IGDT frameworks left this problem unsolved for a generation company to act as either risk-averse or risk-seeker in the market considering benefits/losses obtained from desirable/undesirable variations of multiple uncertain parameters.

Considering the aforementioned discussions, the main contributions of this research work can be summarized as:

1) A new MH-IGDT model for VPP self-scheduling strategy is proposed which neither requires any PDF for uncertain parameters (as in scenario-based programming methods) nor assumes any confidence interval for uncertain parameters (as in robust optimization methods). The proposed MH-IGDT can specifically model and optimize different optimistic/robust uncertainty horizons of multiple uncertain parameters affecting the self-scheduling strategy. It optimally schedules the short-term operation of VPP members both in risk-seeker and risk-averse manners. Accordingly, the risk-averse and risk-seeker Pareto frontiers are provided.

2) For solving the MH-IGDT multi-objective optimization problem, an efficient multi-objective mathematical programming (MOMP) method, i.e., ENNC, is proposed. The proposed ENNC is composed of lexicographic optimization and an augmented version of normalized normal constraint (NNC) method, called hereafter ANNC. Using ANNC, efficient Pareto optimal solutions with uniform distribution in the objective space are generated. Lexicographic optimization approach optimizes ranges of objective functions as well as anchor points in the proposed ENNC to enhance the search efficiency in the objective space.

3) A bi-directional decision-making approach is proposed to find hourly the most preferred Pareto optimal solution for the MH-IGDT problem over the aggregated risk-averse and risk-seeker Pareto sets generated by the ENNC. Thus, unlike the previous uni-directional IGDT-based approaches, the proposed bi-directional decision maker assesses the risk-based behaviors of the VPP in the market and suggests to act as either risk-averse or risk-seeker participant over the scheduling horizon. The proposed decision maker, comprising an ex-ante performance evaluation and forward-backward dynamic programming (FBDP), also optimizes the opportunistic/robustness level of the MH-IGDT model in terms of the uncertainty budget.

The organization of this paper is as follows. In Section II, the proposed MH-IGDT model is introduced. The proposed ENNC method, as a proficient MOMP approach, is presented in Section III. Section IV details the proposed bi-directional decision-making approach. The results obtained from this VPP self-scheduling strategy (comprising MH-IGDT + ENNC + bi-directional decision-making approach) are presented in Section V and compared with the results of other alternatives. Section VI provides the main conclusions.

II. Proposed VPP Self-Scheduling Strategy Model

In this section, the deterministic self-scheduling strategy of VPP for DA market is first introduced briefly. Using it, the proposed MH-IGDT model considering the uncertainty sources is presented.

A. Deterministic VPP Self-Scheduling Strategy

Deterministic self-scheduling strategy for a VPP including dispatchable/non-dispatchable DERs, storages, and loads is as:

$$Max\ \mathcal{F}(\bar{\Theta},\Xi)=\sum_t \mathcal{F}_t(\bar{\Theta},\Xi)= \sum_t\sum_b\left[\bar{\lambda}_{bt}.P^N_{bt}+\sum_{l\in\Omega_{l^b}}\rho_{lt}.\bar{P}_{lt}-\sum_{u\in\Omega_{u^b}}C_u(P_{ut})\right] \quad (1a)$$

$$P^N_{bt}=\sum_{u\in\Omega_{D^b}}P_{ut}+\sum_{u\in\Omega_{S^b}}(P^r_{ut}-P^s_{ut})+\sum_{u\in\Omega_{W^b}}\bar{P}_{ut}-\sum_{l\in\Omega_{l^b}}\bar{P}_{lt} \quad \forall b,\forall t \quad (1b)$$

$$C_u(P_{ut})=A_u.I_{ut}+B_u.P_{ut}+SU^c_u.x_{ut}+SD^c_u.y_{ut} \quad \forall u,\forall t \quad (1c)$$

$$I_{ut}.P^{min}_u\le P_{ut}\le P^{max}_u.I_{ut} \quad \forall u\in\Omega_D,\forall t \quad (1d)$$

$$P_{ut}-P_{u(t-1)}\le RU_u.I_{u(t-1)}+SU^r_u.x_{ut} \quad \forall u\in\Omega_D,\forall t \quad (1e)$$

$$P_{u(t-1)}-P_{ut}\le RD_u.I_{ut}+SD^r_u.y_{ut} \quad \forall u\in\Omega_D,\forall t \quad (1f)$$

$$\sum_{t'=t-\tau^{on}_u+1}^{t}x_{ut'}\le I_{ut} \quad \forall u\in\Omega_D,\forall t \quad (1g)$$

$$\sum_{t'=t-\tau^{off}_u+1}^{t}y_{ut'}\le 1-I_{ut} \quad \forall u\in\Omega_D,\forall t \quad (1h)$$

$$I_{u(t-1)}-I_{ut}+x_{ut}-y_{ut}=0 \quad \forall u\in\Omega_D,\forall t \quad (1i)$$

$$E_{ut}=(1-б_u).E_{u(t-1)}-P^r_{ut}/\mu^r_u+P^s_{ut}.\mu^s_u \quad \forall u\in\Omega_S,\forall t \quad (1j)$$

$$E^{min}_u\le E_{ut}\le E^{max}_u \quad \forall u\in\Omega_S,\forall t \quad (1k)$$

$$E_{ut_{|t=last\ hour\ of\ the\ scheduling\ period}}=E_{u0} \quad \forall u\in\Omega_S \quad (1l)$$

$$0\le P^r_{ut}\le I^r_{ut}.P^{r,max}_u \quad \forall u\in\Omega_S,\forall t \quad (1m)$$

$$0\le P^s_{ut}\le I^s_{ut}.P^{s,max}_u \quad \forall u\in\Omega_S,\forall t \quad (1n)$$

$$I^r_{ut}+I^s_{ut}\le 1 \quad \forall u\in\Omega_S,\forall t \quad (1o)$$

The objective function (1a) maximizes the total profit of VPP coalition, including income of VPP power injection to the contractual buses plus income of selling energy to VPP consumers minus operating costs of VPP units, over the scheduling period. VPP injected power to the grid through each contractual bus is defined in (1b). The operating costs of VPP units are given in (1c). For dispatchable units, all terms of (1c) should be considered, while for wind and storage units (1c) is changed to $C_u(P_{ut})=B_u.P_{ut},\ \forall u\in\Omega_W,\forall t$ and $C_u(P_{ut})=B_u.(P^r_{ut}-P^s_{ut}),\ \forall u\in\Omega_S,\forall t$, respectively. The generation limits of dispatchable units are presented in (1d). Ramping constraints and minimum up/down time limits of dispatchable units are given in (1e)-(1f) and (1g)-(1i), respectively. Although some small-scale dispatchable units have high ramp rates and low MUT/MDT values, the constraints (1e)-(1i) are integrated into the proposed self-scheduling model to keep the comprehensiveness of the model so that it can be applied to VPPs with various coalition units. Dynamic energy balance constraint, energy limits, and end-coupling constraint of storage units are presented in (1j), (1k), and (1l), respectively. The discharging and charging rates are bounded in (1m) and (1n). Simultaneous discharging and charging of storage units are prohibited in (1o).

For the sake of brevity, the deterministic VPP self-scheduling strategy (1a)–(1o) can be recast as follows:

$$\bar{\mathcal{F}}=\underset{\Xi\in\pounds(\bar{\Theta})}{Max}\ \mathcal{F}(\bar{\Theta},\Xi) \quad (2)$$

where the feasible solution space of the deterministic model, i.e., $\pounds(\bar{\Theta})$, is a part of solution space bounded by (1b)–(1o). The solution of this model is just optimal for the forecasted values of the uncertain parameters (i.e., $\bar{\Theta}$), while the uncertain parameters may deviate from their forecasts. To cope with the uncertain parameters, the proposed MH-IGDT model is introduced. Since the deterministic model assumes that the day-ahead forecast values of uncertain parameters would realize the next day, there is no need to consider balancing prices to compensate for excess/deficit power injections in this model.

B. Proposed MH-IGDT Model

IGDT is an interval-based optimization approach which looks for optimizing either robustness against incurring unexpected loss or opportunity of gaining unexpected profit [13]. Thus, based on risk management strategy, the IGDT-based decision-making model can be formulated as either risk-averse or risk-seeker framework. The risk-averse/seeker VPP implements robust/opportunistic function through which the maximum/minimum unfavorable/favorable uncertainty horizons are determined. If the deviation of each uncertain parameter from its forecast falls into its corresponding robust/opportunistic uncertainty horizon, the profit expectations of risk-averse/seeker VPP are guaranteed. Details of single-horizon IGDT method can be found in [13]. Here, the proposed multi-horizon IGDT model is presented.

The forecast-type uncertainties Θ are mathematically formulated through the envelope-bound model in the proposed MH-IGDT framework as follows:

$$\mathcal{R}_\lambda=\left\{\lambda_{bt}:\left|\lambda_{bt}-\bar{\lambda}_{bt}\right|\le\alpha_\lambda.\bar{\lambda}_{bt}\right\} \quad \forall b,\forall t \quad (3a)$$

$$\mathcal{R}_w=\{P_{ut}:|P_{ut}-\bar{P}_{ut}|\le\alpha_w.\bar{P}_{ut}\} \quad \forall u\in\Omega_W,\forall t \quad (3b)$$

$$\mathcal{R}_l=\{P_{lt}:|P_{lt}-\bar{P}_{lt}|\le\alpha_l.\bar{P}_{lt}\} \quad \forall l,\forall t \quad (3c)$$

Considering deviations of uncertain parameters from their forecasts, i.e., $\Delta\Theta$, MH-IGDT model can be constructed from the deterministic counterpart as follows:

$$\mathcal{F}(\bar{\Theta}+\Delta\Theta,\Xi)= \sum_t\sum_b\left[(\bar{\lambda}_{bt}+\Delta\lambda_{bt}).P^N_{bt}+\sum_{l\in\Omega_{l^b}}\rho_{lt}.(\bar{P}_{lt}+\Delta P_{lt})-\sum_{u\in\{\Omega_{D^b}\cup\Omega_{S^b}\}}C_u(P_{ut})-\sum_{u\in\Omega_{W^b}}C_u(\bar{P}_{ut}+\Delta P_{ut})\right] \quad (4)$$

The risk-averse self-scheduling model of VPP is formulated as the following bi-level max-min optimization framework:

$$\underset{\Xi\in\{\pounds(\bar{\Theta}+\Delta\Theta)\cup(5c)\}}{Max}\ (\breve{\alpha}_\lambda,\breve{\alpha}_w,\breve{\alpha}_l) \quad (5a)$$

where

$$\pounds(\bar{\Theta}+\Delta\Theta)=\{(1b)-(1o)\}_{|\bar{\Theta}+\Delta\Theta} \quad (5b)$$

$$\underset{\Delta\Theta}{Min}\ \mathcal{F}(\bar{\Theta}+\Delta\Theta,\Xi)\ge(1-UB).\bar{\mathcal{F}} \quad (5c)$$

subject to:

$$-\breve{\alpha}_\lambda.\bar{\lambda}_{bt}\le\Delta\lambda_{bt}\le\breve{\alpha}_\lambda.\bar{\lambda}_{bt} \quad \forall b,\forall t \quad (5d)$$

$$-\breve{\alpha}_w.\bar{P}_{ut}\le\Delta P_{ut}\le\breve{\alpha}_w.\bar{P}_{ut} \quad \forall u\in\Omega_W,\forall t \quad (5e)$$

$$-\breve{\alpha}_l.\bar{P}_{lt}\le\Delta P_{lt}\le\breve{\alpha}_l.\bar{P}_{lt} \quad \forall l,\forall t \quad (5f)$$

Similarly, the risk-seeker self-scheduling model of VPP is formulated as a bi-level min-max optimization framework as:

$$\underset{\Xi \in \{\pounds(\bar{\theta}+\Delta\theta) \cup (6c)\}}{Min} \ (\hat{\alpha}_\lambda, \hat{\alpha}_w, \hat{\alpha}_l) \quad (6a)$$

where

(5b) (6b)

$$\underset{\Delta\theta}{Max} \ \ \mathcal{F}(\bar{\theta}+\Delta\theta, \Xi) \geq (1+UB).\bar{\mathcal{F}} \quad (6c)$$

subject to:

$$-\hat{\alpha}_\lambda.\bar{\lambda}_{bt} \leq \Delta\lambda_{bt} \leq \hat{\alpha}_\lambda.\bar{\lambda}_{bt} \qquad \forall b, \forall t \quad (6d)$$

$$-\hat{\alpha}_w.\bar{P}_{ut} \leq \Delta P_{ut} \leq \hat{\alpha}_w.\bar{P}_{ut} \qquad \forall u \in \Omega_W, \forall t \quad (6e)$$

$$-\hat{\alpha}_l.\bar{P}_{lt} \leq \Delta P_{lt} \leq \hat{\alpha}_l.\bar{P}_{lt} \qquad \forall l, \forall t \quad (6f)$$

In the bi-level max-min/min-max model (5a)-(5f)/(6a)-(6f), the objective of the upper level (5a)/(6a) is to find the maximum/minimum unfavorable/favorable horizons of uncertainties such that the lower-level objective (5c)/(6c) is satisfied. The control parameter of uncertainty budget (UB) [14] adjusts the risk averting/seeking level of the risk-averse/seeker decision maker. In (5c) and (6c), $\bar{\mathcal{F}}$ is obtained from (2). Details of (5) and (6) can be found in Appendix A.

The upper-level of the risk-averse/seeker models is just a function of Ξ set. The decision variables of the upper-level problem are considered as constant parameters in the lower-level one. Consequently, the lower-level of the risk-averse/seeker models is optimized over $\Delta\theta$ set. The lower-level problems (5c)/(6c) are linear optimization problems where the minimum/maximum of the profit $\mathcal{F}(\bar{\theta}+\Delta\theta, \Xi)$ is obtained on either lower or upper bound of $\Delta\theta$ introduced in (5d)-(5f)/(6d)-(6f). The minimum profit in (5c) is obtained when the locational marginal price (LMP) takes the lowest/highest value during selling/purchasing power to/from the grid as well as the lowest wind generation value and the highest load value occur. Thus, considering (5d)-(5f), constraints (7a)-(7d) derive the minimum profit for the risk-averse model:

$$P^N_{bt}.(\Delta\lambda_{bt} + \breve{\alpha}_\lambda.\bar{\lambda}_{bt}) \leq 0 \qquad \forall b, \forall t \quad (7a)$$

$$P^N_{bt}.(\Delta\lambda_{bt} - \breve{\alpha}_\lambda.\bar{\lambda}_{bt}) \leq 0 \qquad \forall b, \forall t \quad (7b)$$

$$\Delta P_{ut} = -\breve{\alpha}_w.\bar{P}_{ut} \qquad \forall u \in \Omega_W, \forall t \quad (7c)$$

$$\Delta P_{lt} = +\breve{\alpha}_l.\bar{P}_{lt} \qquad \forall l, \forall t \quad (7d)$$

As a result, the equivalent single-level risk-averse MH-IGDT model can be formulated as:

$$\underset{\Xi \in \{\pounds(\bar{\theta}+\Delta\theta)\}}{Max} \ (\breve{\alpha}_\lambda, \breve{\alpha}_w, \breve{\alpha}_l) \quad (8a)$$

subject to:

$$\mathcal{F}(\bar{\theta}+\Delta\theta, \Xi) \geq (1-UB).\bar{\mathcal{F}} \quad (8b)$$

(5b), (5d), (7a)-(7d) (8c)

Similarly, the maximum profit in (6c) is obtained when the LMP takes the highest/lowest value during selling/purchasing power to/from the grid as well as the highest wind generation value and the lowest load value occur. Thus, considering (6d)-(6f), constraints (9a)-(9d) derive the maximum profit for the risk-seeker model:

$$P^N_{bt}.(\Delta\lambda_{bt} + \hat{\alpha}_\lambda.\bar{\lambda}_{bt}) \geq 0 \qquad \forall b, \forall t \quad (9a)$$

$$P^N_{bt}.(\Delta\lambda_{bt} - \hat{\alpha}_\lambda.\bar{\lambda}_{bt}) \geq 0 \qquad \forall b, \forall t \quad (9b)$$

$$\Delta P_{ut} = +\hat{\alpha}_w.\bar{P}_{ut} \qquad \forall u \in \Omega_W, \forall t \quad (9c)$$

$$\Delta P_{lt} = -\hat{\alpha}_l.\bar{P}_{dt} \qquad \forall l, \forall t \quad (9d)$$

As a result, the equivalent single-level risk-seeker MH-IGDT model can be formulated as:

$$\underset{\Xi \in \{\pounds(\bar{\theta}+\Delta\theta)\}}{Min} \ (\hat{\alpha}_\lambda, \hat{\alpha}_w, \hat{\alpha}_l) \quad (10a)$$

subject to:

$$\mathcal{F}(\bar{\theta}+\Delta\theta, \Xi) \geq (1+UB).\bar{\mathcal{F}} \quad (10b)$$

(6b), (6d), (9a)-(9d) (10c)

The nonlinearity of the risk-averse/seeker MH-IGDT scheduling models (8)/(10) arises from the following bilinear terms:

- $\Delta\lambda_{bt}.P^N_{bt}$ in (8b)/(10b),
- $\Delta\lambda_{bt}.P^N_{bt}$ in (8c)/(10c) due to constraints (7a)-(7b)/(9a)-(9b).
- $P^N_{bt}.\breve{\alpha}_\lambda / P^N_{bt}.\hat{\alpha}_\lambda$ in (8c)/(10c) due to constraints (7a)-(7b)/(9a)-(9b).

Thus, the risk-averse/seeker MH-IGDT self-scheduling models do not include highly nonlinear or highly non-convex terms (such as trigonometric functions [15]). Therefore, it is expected that the commercially available non-linear solvers can solve the single-objective problem of each Pareto solution up to global optimality. However, the mathematical proof of this global optimality is out of the scope of this paper.

III. Proposed MOMP Method

The proposed ENNC is composed of ANNC and lexicographic optimization, which are introduced in the following.

NNC is a well-organized MOMP method that provides uniformly distributed Pareto optimal solutions for a multi-objective optimization problem by reducing the feasible objective space systematically [16]. Despite the NNC capability to cover various parts of the objective space, it suffers from generating inefficient or dominated solutions. To remedy this problem, ANNC has been presented in [17], which augments the Pareto solution production mechanism of NNC using slack variables. ANNC can essentially generate solely non-dominated or efficient Pareto solutions. At the same time, ANNC saves the advantages of NNC to search objective space systematically and to generate distributed Pareto solutions uniformly. Details of ANNC can be found in [17].

The second component of the proposed ENNC is lexicographic optimization [18]. In [19], lexicographic optimization has been used to successively optimize the objective functions of a multi-objective problem. In [20], the range of objective functions in an augmented ε-constraint method has been optimized by lexicographic optimization. However, lexicographic optimization has been used in our proposed MOMP approach to 1) optimize the payoff matrixes of risk-averse/seeker MH-IGDT models with corresponding lexicographic orders, and 2) optimize the risk-averse/seeker anchor points of the ENNC method, which leads to improving the ENNC search efficiency in the objective space. The performance of the lexicographic optimization to construct the payoff matrix of the risk-averse MH-IGDT problem is as follows.

In order to obtain the first row of the risk-averse payoff matrix, the uncertainty horizons are sorted as lexicographic order $\{\breve{\alpha}_\lambda, \breve{\alpha}_w, \breve{\alpha}_l\}$:

$$\text{Step 1)} \ \breve{\alpha}^*_\lambda = \underset{\Xi \in \{\pounds(\bar{\theta}+\Delta\theta)\} \cap (8b) \cap (8c)}{Max} \breve{\alpha}_\lambda \quad (11a)$$

$$\text{Step 2)} \ \breve{\alpha}^*_w = \underset{\Xi \in \{\{\pounds(\bar{\theta}+\Delta\theta)\} \cap (8b) \cap (8c)\}|_{\breve{\alpha}_\lambda = \breve{\alpha}^*_\lambda}}{Max} \breve{\alpha}_w \quad (11b)$$

$$\text{Step 3)} \ \breve{\alpha}^*_l = \underset{\Xi \in \{\{\pounds(\bar{\theta}+\Delta\theta)\} \cap (8b) \cap (8c)\}\Big|_{\substack{\breve{\alpha}_\lambda = \breve{\alpha}^*_\lambda \\ \breve{\alpha}_w = \breve{\alpha}^*_w}}}{Max} \breve{\alpha}_l \quad (11c)$$

As (11) implies, Step 1 gives the diagonal element while Steps 2 and 3 form off-diagonal elements of the first row of this

payoff matrix. The second and third rows of the risk-averse payoff matrix are obtained using the three-step procedure presented in (11) with lexicographic orders $\{\breve{\alpha}_w, \breve{\alpha}_l, \breve{\alpha}_\lambda\}$ and $\{\breve{\alpha}_l, \breve{\alpha}_\lambda, \breve{\alpha}_w\}$, respectively. While the payoff matrix in NNC and ANNC methods is constructed by just substituting the single-objective optimization solution of an objective function in the other ones [18], the risk-averse payoff matrix in (11) is constructed by individually optimizing each uncertainty horizon considering the results obtained for the previous ones. These optimized ranges of objective functions enhance search efficiency of the proposed ENNC in the objective space.

To construct the optimized payoff matrix for the risk-seeker MH-IGDT problem, the same procedure is followed except for (11) which is changed as (12):

$$\text{Step 1)}\ \hat{\alpha}_\lambda^* = \underset{\Xi \in \{\pounds(\bar{\theta}+\Delta\theta)\}\cap(10b)\cap(10c)}{Min} \hat{\alpha}_\lambda \tag{12a}$$

$$\text{Step 2)}\ \hat{\alpha}_w^* = \underset{\Xi \in \{\{\pounds(\bar{\theta}+\Delta\theta)\}\cap(10b)\cap(10c)\}_{|\hat{\alpha}_\lambda=\hat{\alpha}_\lambda^*}}{Min} \hat{\alpha}_w \tag{12b}$$

$$\text{Step 3)}\ \hat{\alpha}_l^* = \underset{\Xi \in \{\{\pounds(\bar{\theta}+\Delta\theta)\}\cap(10b)\cap(10c)\}_{\left|\begin{smallmatrix}\hat{\alpha}_\lambda=\hat{\alpha}_\lambda^*\\ \hat{\alpha}_w=\hat{\alpha}_w^*\end{smallmatrix}\right.}}{Min} \hat{\alpha}_l \tag{12c}$$

In addition to optimizing the payoff matrix, using the proposed lexicographic orders and lexicographic optimizations, the anchor points of the ANNC [17] are also optimized within the proposed ENNC. In other words, each anchor point coordinate in the objective space (which is one objective function in the MH-IGDT problem) is successively optimized considering the results obtained for the previous coordinates. Since the anchor points are the vertices of the utopia hyperplane in the objective space, this feature provides a more effective utopia hyperplane for the ENNC to generate the Pareto frontier. However, only one coordinate is optimized for each anchor point in the ANNC.

IV. Bi-directional Decision-Making Framework

The proposed bi-directional decision-making approach: a) selects the most profitable Pareto solution within the risk-averse/seeker Pareto sets considering various realizations of the uncertain parameters, b) fine-tunes UB setting for the risk-averse/seeker MH-IGDT models, c) addresses the unsolved problem of acting as risk-averse or risk-seeker VPP in the market. The proposed decision maker includes an ex-ante performance evaluation method and an FBDP approach.

A. Ex-ante Performance Evaluation Method

The proposed ex-ante performance evaluation method assesses risk-averse/seeker Pareto solutions provided by the proposed ENNC using various realizations of the uncertain parameters. The performance of this method, which acts before the actual realization of the uncertain parameters, is as follows:

Step 1) A sufficient number of scenarios are generated by the ARMA-based scenario generation method of [21]. Each scenario includes one realization of Θ over the scheduling period. To implement a fair comparison, the same performance evaluation scenarios (in-sample scenarios) are used for all Pareto solutions.

Step 2) Initialize the Pareto solution counter $j = 1$. Also, set UB value.

Step 3) Initialize scenario counter $\zeta = 1$.

Step 4) Set all uncertain parameters of Θ based on the realized values in scenario ζ.

Step 5) All decision variables Ξ are partitioned to scenario-independent variables $\Xi^j = \{I_{ut}^j, x_{ut}^j, y_{ut}^j\}$, $\forall u \in \Omega_D, \forall j, \forall t$ and scenario-dependent variables $\Xi^{j\zeta} = \{P_{ut}^{j\zeta}, \forall u \in \Omega_D, (I_{ut}^{r,j\zeta}, I_{ut}^{s,j\zeta}, P_{ut}^{r,j\zeta}, P_{ut}^{s,j\zeta}), \forall u \in \Omega_S\}$, $\forall j, \forall \zeta, \forall t$. The variables Ξ^j are fixed based on the results of Pareto solution j. However, $\Xi^{j\zeta}$ variables are separately determined for each scenario ζ of Pareto solution j, since these decision variables can be easily changed in the real-time operation. In this way, the performance of each Pareto optimal solution j encountering various realizations of the uncertain parameters can be evaluated.

Step 6) For each scenario ζ, the following optimization problem is solved to determine its $\mathcal{F}^{j\zeta}$:

$$Max\ \mathcal{F}^{j\zeta}(\Theta^\zeta, \Xi) = \sum_t \mathcal{F}_t^{j\zeta}(\Theta^\zeta, \Xi) = \sum_t \sum_b \left[\lambda_{bt}^\zeta . P_{bt}^{N,j} + \sum_{l \in \Omega_{lb}} \rho_{lt} . P_{lt}^\zeta - \sum_{u \in \Omega_{ub}} C_u(P_{ut}^{j\zeta}) + \lambda_{bt}^{\zeta,+} . \Delta P_{bt}^{N,j\zeta,+} - \lambda_{bt}^{\zeta,-} . \Delta P_{bt}^{N,j\zeta,-}\right] \quad \forall\zeta, \forall j \tag{13a}$$

$$P_{bt}^{N,j\zeta} = \sum_{u \in \Omega_{Db}} P_{ut}^{j\zeta} + \sum_{u \in \Omega_{sb}} (P_{ut}^{r,j\zeta} - P_{ut}^{s,j\zeta}) + \sum_{u \in \Omega_{Wb}} P_{ut}^\zeta - \sum_{l \in \Omega_{lb}} P_{lt}^\zeta \quad \forall b, \forall t, \forall\zeta, \forall j \tag{13b}$$

$$C_u(P_{ut}^{j\zeta}) = A_u . I_{ut}^j + B_u . P_{ut}^{j\zeta} + SU_u^c . x_{ut}^j + SD_u^c . y_{ut}^j \quad \forall u, \forall t, \forall\zeta, \forall j \tag{13c}$$

$$I_{ut}^j . P_u^{min} \le P_{ut}^{j\zeta} \le P_u^{max} . I_{ut}^j \quad \forall u \in \Omega_D, \forall t, \forall\zeta, \forall j \tag{13d}$$

$$P_{ut}^{j\zeta} - P_{u(t-1)}^{j\zeta} \le RU_u . I_{u(t-1)}^j + SU_u^r . x_{ut}^j \quad \forall u \in \Omega_D, \forall t, \forall\zeta, \forall j \tag{13e}$$

$$P_{u(t-1)}^{j\zeta} - P_{ut}^{j\zeta} \le RD_u . I_{ut}^j + SD_u^r . y_{ut}^j \quad \forall u \in \Omega_D, \forall t, \forall\zeta, \forall j \tag{13f}$$

$$\sum_{t'=t-\tau_u^{on}+1}^{t} x_{ut'}^j \le I_{ut}^j \quad \forall u \in \Omega_D, \forall t, \forall j \tag{13g}$$

$$\sum_{t'=t-\tau_u^{off}+1}^{t} y_{ut'}^j \le 1 - I_{ut}^j \quad \forall u \in \Omega_D, \forall t, \forall j \tag{13h}$$

$$I_{u(t-1)}^j - I_{ut}^j + x_{ut}^j - y_{ut}^j = 0 \quad \forall u \in \Omega_D, \forall t, \forall j \tag{13i}$$

$$E_{ut}^{j\zeta} = (1 - \delta_u) . E_{u(t-1)}^{j\zeta} - P_{ut}^{r,j\zeta}/\mu_u^r + P_{ut}^{s,j\zeta} . \mu_u^s \quad \forall u \in \Omega_S, \forall t, \forall\zeta, \forall j \tag{13j}$$

$$E_u^{min} \le E_{ut}^{j\zeta} \le E_u^{max} \quad \forall u \in \Omega_S, \forall t, \forall\zeta, \forall j \tag{13k}$$

$$E_{ut_{|t=last\ hour\ of\ the\ scheduling\ period}}^{j\zeta} = E_{u0}\ \forall u \in \Omega_S, \forall\zeta, \forall j \tag{13l}$$

$$0 \le P_{ut}^{r,j\zeta} \le I_{ut}^{r,j\zeta} . P_u^{r,max} \quad \forall u \in \Omega_S, \forall t, \forall\zeta, \forall j \tag{13m}$$

$$0 \le P_{ut}^{s,j\zeta} \le I_{ut}^{s,j\zeta} . P_u^{s,max} \quad \forall u \in \Omega_S, \forall t, \forall\zeta, \forall j \tag{13n}$$

$$I_{ut}^{r,j\zeta} + I_{ut}^{s,j\zeta} \le 1 \quad \forall u \in \Omega_S, \forall t, \forall\zeta, \forall j \tag{13o}$$

$$\Delta P_{bt}^{N,j\zeta,+} - \Delta P_{bt}^{N,j\zeta,-} = P_{bt}^{N,j\zeta} - P_{bt}^{N,j} \quad \forall b, \forall t, \forall\zeta, \forall j \tag{13p}$$

$$0 \le \Delta P_{bt}^{N,j\zeta,+} \le (1 - z_{bt}^{j\zeta}) . (P_{bt}^{N,j\zeta} - P_{bt}^{N,j}) \quad \forall b, \forall t, \forall\zeta, \forall j \tag{13q}$$

$$0 \le \Delta P_{bt}^{N,j\zeta,-} \le z_{bt}^{j\zeta} . (P_{bt}^{N,j} - P_{bt}^{N,j\zeta}) \quad \forall b, \forall t, \forall\zeta, \forall j \tag{13r}$$

The first three terms in the objective (13a) are similar to the three terms in (1a). However, the forecasts of the uncertain parameters, i.e., $\bar{\lambda}_{bt}$, $\bar{P}_{ut}$, $\forall u \in \Omega_W$, and $\bar{P}_{lt}$, are replaced by the realized values for these uncertain parameters in scenario ζ, i.e., λ_{bt}^ζ, P_{ut}^ζ, $\forall u \in \Omega_W$, and P_{lt}^ζ. In addition, P_{bt}^N and P_{ut} are replaced by $P_{bt}^{N,j\zeta}$ and $P_{ut}^{j\zeta}$. The next two terms of (13a) model sell/purchase of excess/deficit injected power to the grid with respect to the scheduled value in the Pareto solution j. These excess/deficit values are denoted by $\Delta P_{bt}^{N,j\zeta,+}/\Delta P_{bt}^{N,j\zeta,-}$ and their prices are shown by $\lambda_{bt}^{\zeta,+}/\lambda_{bt}^{\zeta,-}$. Thus, (13a) models the realized profit of the Pareto solution j in scenario ζ, i.e., $\mathcal{F}^{j\zeta}(\Theta^\zeta, \Xi)$,

considering the realized values for the uncertain parameters in scenario ζ, i.e., Θ^{ζ}. Constraints (13b)-(13p) are similar to (1b)-(1p) considering the variables' dependencies on scenario ζ and Pareto solution j. Constraints (13p)-(13r) model $\Delta P_{bt}^{N,j\zeta,+}$/ $\Delta P_{bt}^{N,j\zeta,-}$ where $z_{bt}^{j\zeta}$ is a binary modeling variable to determine the excess/deficit injected power to the grid. In these constraints, $P_{bt}^{N,j}$ indicates the scheduled value for P_{bt}^{N} in Pareto solution j and $P_{bt}^{N,j\zeta}$ is the obtained value for $P_{bt}^{N,j}$ in scenario ζ through the optimization problem (13) considering the uncertainties' realizations in scenario ζ. The only nonlinearity in (13) is related to the product $z_{bt}^{j\zeta}.P_{bt}^{N,j\zeta}$ in (13q) and (13r). This nonlinear term can be linearized using the big-M linearization method as:

$$0 \le \Delta P_{bt}^{N,j\zeta,+} \le P_{bt}^{N,j\zeta} - P_{bt}^{N,j} - LP_{bt}^{N,j\zeta} + z_{bt}^{j\zeta}.P_{bt}^{N,j} \quad \forall b,\forall t,\forall \zeta,\forall j \quad (14a)$$

$$0 \le \Delta P_{bt}^{N,j\zeta,-} \le z_{bt}^{j\zeta}.P_{bt}^{N,j} - LP_{bt}^{N,j\zeta} \quad \forall b,\forall t,\forall \zeta,\forall j \quad (14b)$$

$$-M.z_{bt}^{j\zeta} \le LP_{bt}^{N,j\zeta} \le M.z_{bt}^{j\zeta} \quad \forall b,\forall t,\forall \zeta,\forall j \quad (14c)$$

$$P_{bt}^{N,j\zeta} - M.\left(1 - z_{bt}^{j\zeta}\right) \le LP_{bt}^{N,j\zeta} \le P_{bt}^{N,j\zeta} + M.\left(1 - z_{bt}^{j\zeta}\right) \quad \forall b,\forall t,\forall \zeta,\forall j \quad (14d)$$

where $LP_{bt}^{N,j\zeta}$ is an auxiliary continuous variable used for linearization. The formulation (14a)-(14d) is the exact linearized form of the nonlinear constraints (13q) and (13r). Thus, the nonlinear optimization problem (13a)-(13r) is linearized as (13a)-(13p) and (14a)-(14d). Since this optimization problem should be solved for all scenarios ζ, solving this problem is the most time-consuming part of the proposed solution method, and thus, its linearization significantly reduces the computation burden of the proposed method.

Step 7) If ζ is less than the number of scenarios, set $\zeta = \zeta + 1$ and return to Step 4; otherwise, calculate the expected profit of Pareto solution j as the expected value of $\mathcal{F}^{j\zeta}$ values over the generated scenarios ζ.

Step 8) If j is less than the number of Pareto solutions, set $j = j + 1$ and go back to Step 3; otherwise, find the most profitable Pareto solution having the highest expected profit value (obtained in the previous step) and report it.

The aforementioned eight-step performance evaluation method is implemented separately over risk-averse/seeker Pareto sets to attain the most profitable risk-averse/seeker Pareto solutions for each particular value of UB. In addition, this method is run for different UB values. In this way, a set of most profitable risk-averse/seeker Pareto solutions over various UB values is produced. Using this set, the final solution of the VPP self-scheduling problem is constructed by the proposed FBDP approach.

The proposed ex-ante performance evaluation method uses scenarios through a different way compared to stochastic programming. While stochastic programming uses scenarios to model uncertainties, the ex-ante performance evaluation uses in-sample scenarios to select the most profitable Pareto solution within the generated Pareto set considering various realizations of uncertain parameters. However, any other decision maker that does not require these scenarios, such as optimality-based decision maker [22] and fuzzy decision maker [23], can be used instead of the ex-ante performance evaluation method. In addition, since the performance of the whole proposed hybrid methodology is less sensitive to these in-sample scenarios than scenario-based approaches, we can generate scenarios of the ex-ante performance evaluation method without using PDF of uncertain parameters. For instance, in the practical power systems, we can use historical data (i.e., previous realizations) of uncertain parameters, recorded in the SCADA (supervisory control and data acquisition) systems, as the in-sample scenarios for the ex-ante performance evaluation method.

B. FBDP

The most profitable Pareto optimal solution in the previous subsection is attained assuming that the VPP owner takes solely risk-averse/seeker role in the market with a fixed robustness/opportunistic level for all the scheduling hours. However, market conditions and uncertain parameters usually change from hour to hour. Thus, hourly decision making to act as either risk-averse or risk-seeker player and to select appropriate robustness or opportunistic level (in terms of UB value) can provide higher profit for the VPP. The proposed FBDP addresses this critical issue considering the VPP inter-temporal constraints.

In the proposed FBDP, the stages are scheduling hours and the states of each stage represent the results of the most profitable risk-averse/seeker Pareto optimal solutions with different UB values in that hour as shown in Fig. 1. In this figure, 24 scheduling hours from $t = 1$ to $t = 24$ and 11 states from $k = 1$ to $k = 11$ are shown. These 11 states include five most profitable risk-seeker, one risk-neutral (i.e., deterministic), and five most profitable risk-averse Pareto optimal solutions. In the five most profitable risk-averse/seeker Pareto optimal solutions (denoted by $\check{\pi}^{*}$and $\hat{\pi}^{*}$, respectively), $UB = 10\%$ to $UB = 50\%$ are considered, while the risk-neutral deterministic solution (denoted by $\bar{\pi}^{*}$) is specified by $UB = 0$ as shown in Fig. 1. The proposed FBDP seeks the most profitable path in the forward movement. However, from each stage to the next one, the VPP inter-temporal constraints should be checked due to the probable change of the Pareto solution. If a violation from the inter-temporal constraints occurs, the FBDP through the backward movement returns to the switching stage that causes the infeasibility and does not make that switching action. An instance of backward movement is illustrated by red color in Fig. 1 where switching from state 5 in stage 2 to state 6 in stage 3 causes a violation from the VPP inter-temporal constraints (e.g., violation from the minimum up/down time limits). Thus, the FBDP returns from state 6 in stage 3 to state 5 in stage 2. The inter-temporal constraints here include the dynamic energy balance constraints (1j) and other relevant constraints (1k)-(1l) of storage units as well as the ramping constraints (1e)-(1f) and minimum up/down time limits (1g)-(1i) of dispatchable units. The proposed FBDP performs based on the following steps:

Step 1) Initialize the stage counter, $t = 0$. The state of this stage is known from the last hour of the previous scheduling day.

Step 2) In each stage t with state k, find more profitable states for switching in the next stage t+1. These states are indexed by k'. If there is no state k', remain in state k in the next stage t+1 (i.e., no switching action is performed) and go to Step 4. Otherwise, sort the more profitable states k' in terms of their profits.

Step 3) Begin with the most profitable state k'. If switching from k to k' is feasible (i.e., it does not violate the inter-tem-

poral constraints in the next stage), perform this switching action and update the profit as well as the energy level of storage units based on the new state k'. Otherwise, this switching action is not feasible and evaluate the second most profitable state k'. This cycle is repeated until:

3-1) No feasible state k' is found. In this case, the proposed FBDP remains in the same state k in the next stage t+1.

3-2) A feasible state k' is found. In this case, the proposed FBDP switches from state k in stage t to state k' in stage t+1.

Step 4) $t = t$+1. If t < 24, go to Step 2. Otherwise, the most profitable and feasible states of all time stages have been determined and thus report the final solution of the VPP self-scheduling problem.

Using the forward and backward movements, the proposed FBDP can find the economically optimal and technically feasible (regarding inter-temporal constraints) self-schedule for the VPP. Even if a VPP has no inter-temporal constraint, the backward movements of the FBDP may not be required. However, the FBDP using its forward movements can still find the most profitable self-scheduling strategy to act as either risk-averse or risk-seeker participant and to decide the risk-averting/seeking level for each hour of the self-scheduling horizon.

It is noted that the proposed FBDP does not suffer from the curse of dimensionality problem occurred in solving unit commitment by DP. The states of the proposed FBDP are risk-averse/neutral/seeker Pareto optimal solutions and not unit combinations. While the number of unit combinations in a unit commitment problem increases exponentially with the number of units, the number of states in each stage of the proposed FBDP increases linearly with the number of UB levels. For instance, there are 11 UB levels in Fig. 1. If we have 11 units in a unit commitment problem, we would have $2^{11}-1=2047$ states in each stage of its DP [24], while 11 UB levels lead to 11 states in each stage of the proposed FBDP.

V. Numerical Results

The effectiveness of the proposed VPP self-scheduling strategy (including MH-IGDT, ENNC, and bi-directional decision maker) is illustrated on a coalition of dispatchable and non-dispatchable units.

The dispatchable units contain two 12-MW oil/steam units, one 20-MW oil/combined turbine type unit, and one 5-MW storage unit. The data of the two 12-MW and one 20-MW units is taken from the IEEE-RTS [25] which is shown in Table B1 in Appendix B. The data of the storage unit is given in Table I. It is assumed that the storage unit has no stored energy at the start of the 24-hour scheduling horizon. Also, one 50-MW wind farm is a member of the coalition. The cut-in, rated, and cut-out speeds of the wind farm are 3, 14, and 25 m/s, respectively. Moreover, it is assumed that 20% of hourly load pertaining to bus 2 of the IEEE-RTS [25] is a member of the VPP. The LMP forecasts and the load price used for the VPP test case are graphically illustrated in Fig. 2. The load consumption price in Fig. 2 is 60 \$/MWh. Besides, the forecasts of load and wind speed, used for this test case, are shown in Fig. 3.

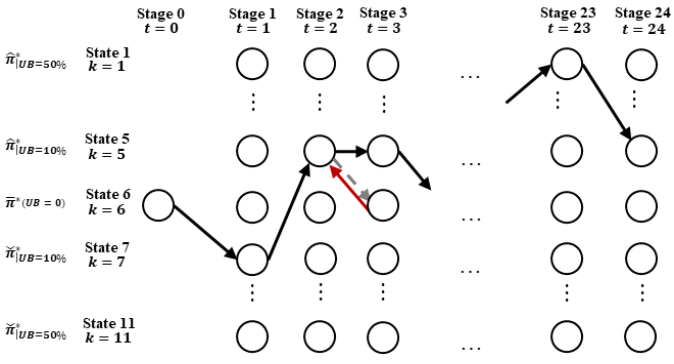

Fig. 1. Illustration of the proposed FBDP.

The vector of uncertain parameters Θ includes one load, one wind generation, and one LMP pertaining to the contractual bus. The historical data of these uncertain parameters is obtained from the hourly data related to the Millwood City in New York, US from Oct.1, 2014 to Nov. 4, 2015 [26], [27]. The forecast values of these uncertain parameters are related to Nov. 5, 2015. The big-M values in (14c) and (14d) should be: $M \geq \left|P_{bt}^{N,j\zeta}\right|$. In this test case, the big-M values are set to 100MW, which is the minimum value satisfying this condition.

The optimal solution results of the proposed VPP self-scheduling strategy are first provided and analyzed. Then, comparative results for the proposed model and the proposed solution method are presented. All case studies of this paper have been run on a 64-bit core i7 2.40 GHz personal computer with 4 GB RAM. The proposed MH-IGDT model is an MINLP optimization problem. Its nonlinear nature arises by the bilinear terms introduced in Subsection II.B. Thus, this model should be solved by an MINLP solver, such as DICOPT [28] used in this paper. However, the ex-ante performance evaluation method has an MILP formulation. Thus, the optimization problems of

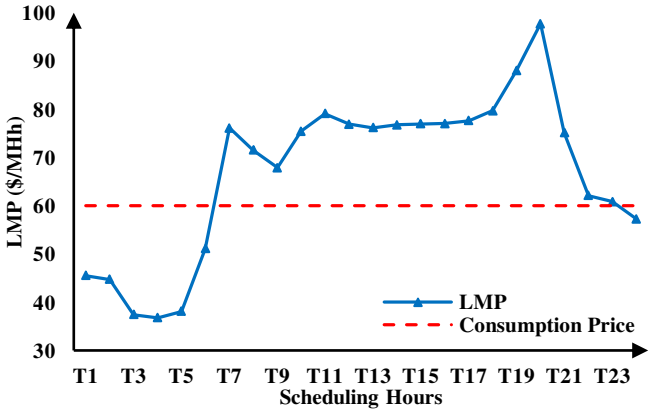

Fig. 2. LMP forecast and consumption price for the VPP test case.

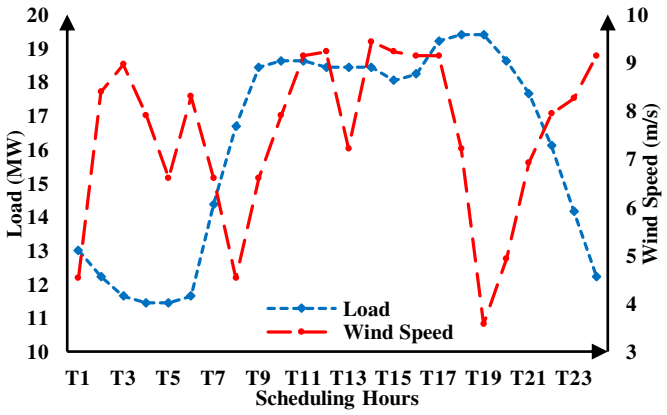

Fig. 3. Load forecast and wind speed forecast for the VPP test case.

TABLE I
THE STORAGE UNIT DATA SET

$б_u$	μ_u^r, μ_u^s	E_u^{min}, E_u^{max} (MWh)
0.03	0.85, 0.90	0, 100

this method can be solved by an MILP solver, such as CPLEX [28] used in this paper. The MINLP optimization problem of the proposed MH-IGDT model has small size since it is solved solely for the worst-case realization of uncertain parameters. Thus, this MINLP problem can be easily solved. On the other hand, although the ex-ante performance evaluation method includes various realizations of uncertain parameters, its optimization problems have MILP form which can be tractably solved. Thus, the whole proposed VPP self-scheduling approach has a tractable computation burden.

Fig. 2 shows that the consumption price is lower than the LMP in most of the scheduling hours. Thus, selling VPP produced power to the grid is overall more profitable than selling it to the load. Accordingly, the VPP minimum profit in (5c) is obtained when the highest load occurs based on (7d). The data of the generated scenarios for the ex-ante performance evaluation method are given in Appendix B.

A. *Optimal Solution Results*

The proposed risk-averse/seeker MH-IGDT + ENNC approach is evaluated for 10 MH-IGDT cases and one deterministic case. The 10 MH-IGDT cases include five risk-seeker models with $UB = 50\%, 40\%, 30\%, 20\%$, and 10% (specified by $k = 1, 2, 3, 4$, and 5, respectively) as well as five risk-averse cases with $UB = 10\%, 20\%, 30\%, 40\%$, and 50% (specified by $k = 7, 8, 9, 10$, and 11, respectively). The risk-neutral deterministic case with $UB = 0\%$ is specified by $k = 6$. In other words, the models are sorted from the most risk-seeker case ($k = 1$) to risk-neutral deterministic case ($k = 6$) and to the most risk-averse case ($k = 11$). For each of these 11 models (i.e., $k = 1$ to $k = 11$), 45 Pareto solutions are generated by the proposed ENNC. For instance, the uncertainty horizons $\breve{\alpha}_\lambda$, $\breve{\alpha}_w$, $\breve{\alpha}_l$ obtained by the 45 Pareto solutions of the risk-averse model with $UB = 20\%$ (i.e., the eighth model or $k = 8$) are shown in Fig. 4. These 45 Pareto solutions are indicated by J1 to J45 on the horizontal axis of Fig. 4, and the vertical axis indicates $\breve{\alpha}_\lambda$, $\breve{\alpha}_w$, and $\breve{\alpha}_l$ values of these solutions. This figure shows that $\breve{\alpha}_\lambda$, $\breve{\alpha}_w$, and $\breve{\alpha}_l$ vary in the ranges [0, 0.1107], [0, 0.3123], and [0, 0.7473], respectively, in the 45 Pareto solutions of the eighth model. As an example, $\breve{\alpha}_\lambda$, $\breve{\alpha}_w$, and $\breve{\alpha}_l$ in the first Pareto solution J1 of Fig. 4 are 0.1107, 0.0168, and 0.0874, respectively. This means that the profit obtained by Pareto solution J1 is robust as long as the uncertain parameters' deviations from their forecast values are $\left|\lambda_{bt}^{\zeta} - \bar{\lambda}_{bt}\right| \le 0.1107\bar{\lambda}_{bt}$, $\bar{P}_{ut} - P_{ut}^{\zeta} \le 0.0168\bar{P}_{ut}$, $\forall u \in \Omega_W$ and $P_{lt}^{\zeta} - \bar{P}_{lt} \le 0.0874\bar{P}_{lt}$. In the risk-averse models, the worst LMP value can be on both sides of its forecast value as specified in (7a)-(7b). However, the worst wind and load values can only be on one side of their forecast values as specified in (7c) and (7d). Thus, the absolute value operator has been only used for the price deviations. Another point which can be seen from Fig. 4 is the higher dependency of the VPP profit on LMP, then wind generation, and finally load as a lower variation of LMP (and then wind generation and finally load) consumes the entire uncertainty budget.

The 24-hour profits of the 45 Pareto solutions pertaining to risk-seeker model with $UB = 20\%$ ($k = 4$), risk-neutral deterministic model with $UB = 0$ ($k = 6$), and risk-averse model with $UB = 20\%$ ($k = 8$), calculated using the proposed ex-ante performance evaluation method, are shown in Fig. 5. In the deterministic model with $UB = 0$, the uncertainty horizons become zero in all 45 Pareto solutions. Thus, the same profit is obtained in all Pareto solutions of this deterministic model, as shown in Fig. 5. In this figure, all the Pareto solutions of the risk-averse model and most of the Pareto solutions of the risk-seeker model have higher profits than the deterministic model. In addition, the profits of the Pareto solutions of the risk-seeker model show higher variations than the profits of the Pareto solutions of the risk-averse model. The best Pareto solution of the risk-averse and the risk-seeker model is J3 and J27, respectively, indicated by the surrounding circle in Fig. 5.

The VPP self-scheduling strategy obtained by the proposed FBDP is shown in Fig. 6. The best Pareto optimal solutions of the 11 models are the states of the FBDP and 24 hours of the scheduling day are the stages of the FBDP, which are shown vertically and horizontally in Fig. 6, respectively. The proposed FBDP approach searches for the most profitable and feasible path among risk-seeker/neutral/averse states over the scheduling horizon such that the VPP inter-temporal constraints are satisfied. In this path, the forward and backward movements are illustrated by blue and red arrows in Fig. 6, respectively.

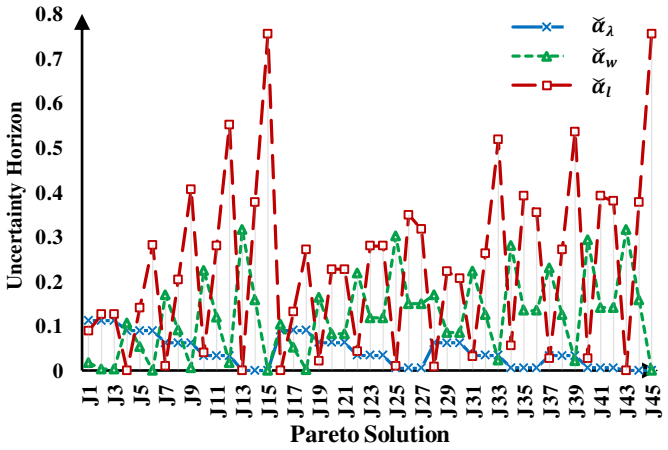

Fig. 4. The uncertainty horizons obtained by the 45 Pareto solutions of the risk-averse model with UB=20%.

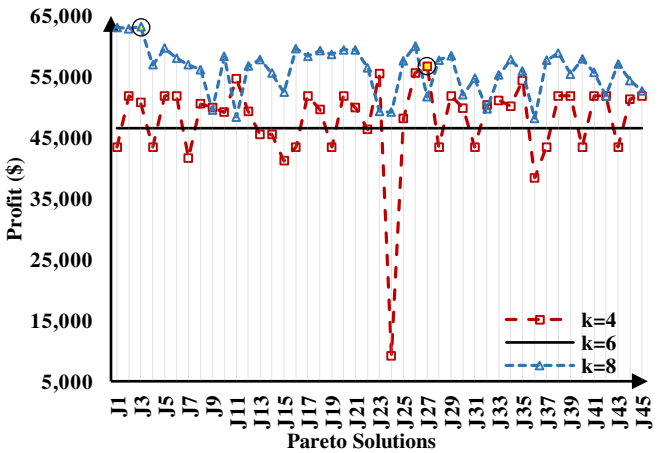

Fig. 5. The 24-hour profits of the 45 Pareto optimal solutions pertaining to the fourth, sixth, and eighth models.

According to this figure, the proposed FBDP selects the risk-seeker states during hours 3-6 and 22-24 to benefit from favorable variations of uncertain parameters. Discussing in more details, the risk-seeker states are chosen in hours with low LMP and load values and high wind generation values aiming that the VPP takes the advantages of wind generation deviations above the $\bar{P}_{ut}, \forall u \in \Omega_W$ without serious concern for the deviations below the forecasts due to the low cost of supply from the grid. By further increasing the wind generation and decreasing the LMP and load in these hours, the risk-seeking level of the VPP increases (e.g., in hour 3). Alternatively, by tending to be robust at unfavorable realizations of the uncertain parameters, the risk-averse states are selected in hours 1-2 and 7-21 with high LMP and load values. Since both the VPP load and the cost of supplying it from the grid are high, a risk-averse self-scheduling strategy is adopted by the proposed FBDP in these hours to avoid serious economic risks.

Three backward movements are seen in Fig. 6 due to violating the VPP inter-temporal constraints. The first two ones occur at hour 2 due to violating the minimum up-time constraint of one 12-MW unit. At first, the proposed FBDP switches back from state 4 in stage 2 to state 7 in stage 1 due to this violation. Switching to the next most profitable state (i.e., state 5) leads to the same violation, yielding the second backward transition. Thus, the FBDP moves to the next most profitable state 8 in stage 2, which is feasible in terms of the minimum up-time constraint. Also, violating the end-coupling constraint of the 5-MW storage unit leads to the third backward movement of the FBDP in hour 24 to remain in state 5.

The execution time of the whole proposed VPP self-scheduling strategy (i.e., MH-IGDT + ENNC + ex-ante performance evaluation + FBDP) for this test case is about 8 minutes (exactly 7:58 min), which is a completely acceptable computation time for a day-ahead self-scheduling problem.

B. Comparative Results of Solution Methods

To better illustrate the performance of the proposed FBDP self-scheduling strategy, the 24-hour profit of the FBDP solution is compared with the 24-hour profit of the most profitable Pareto solutions of the 11 risk seeker/neutral/averse models in Table II. It is seen that the proposed FBDP attains the highest profit in Table II, illustrating its effectiveness. The reason for this better performance is bi-directional decision making of the proposed FBDP considering both risk-seeker and risk-averse behaviors. Moreover, the proposed FBDP can adaptively select the best risk-seeking/averting level in each hour based on the uncertain parameters' realizations. However, the 11 comparative models can only adopt risk seeker/neutral/averse decision making with a fixed UB over the scheduling horizon.

In Table III, the proposed ENNC is compared with other MOMP methods including weighted sum (WS) [29], normal boundary intersection (NBI) [30], NNC [16], modified augmented ε-constraint (MAEC) [31], and ANNC [17]. To fairly compare the MOMP methods of Table III, the same ex-ante performance evaluation and FBDP have been used for all of these methods. Moreover, 45 Pareto solutions have been considered for these methods except for WS, which can essentially produce only one Pareto optimal solution. For this reason, WS has the poorest performance among the MOMP methods of Table III. NBI and NNC generate a set of Pareto solutions with uniform distribution and thus have considerably better performance than WS. However, NNC is less prone to produce dominated Pareto solutions than NBI [16], which leads to its higher profit in Table III. MAEC only generates non-dominated Pareto solutions, and thus, it has better performance than NBI and NNC in Table III. ANNC both generates non-dominated Pareto solutions and distributes these solutions uniformly in the objective space. Therefore, ANNC obtains a higher profit than MAEC. The proposed ENNC has the advantages of ANNC in addition to optimizing the payoff matrix to attain the optimal ranges of the uncertainty horizons as well as optimizing the anchor points to provide a more effective utopia hyperplane. Due to these reasons, the proposed ENNC has the best performance among the MOMP methods of Table III.

To further evaluate the effectiveness of the proposed VPP self-scheduling strategy, it is compared with:

- Two-stage stochastic programming (SP) with three different numbers of scenarios in Table IV [3], [4]. These SP methods, denoted by SP1, SP2, and SP3, have 20, 50, 100 scenarios.
- First-order stochastic dominance (FOSD) with three different numbers of benchmark scenarios in Table V [32]. These FOSD

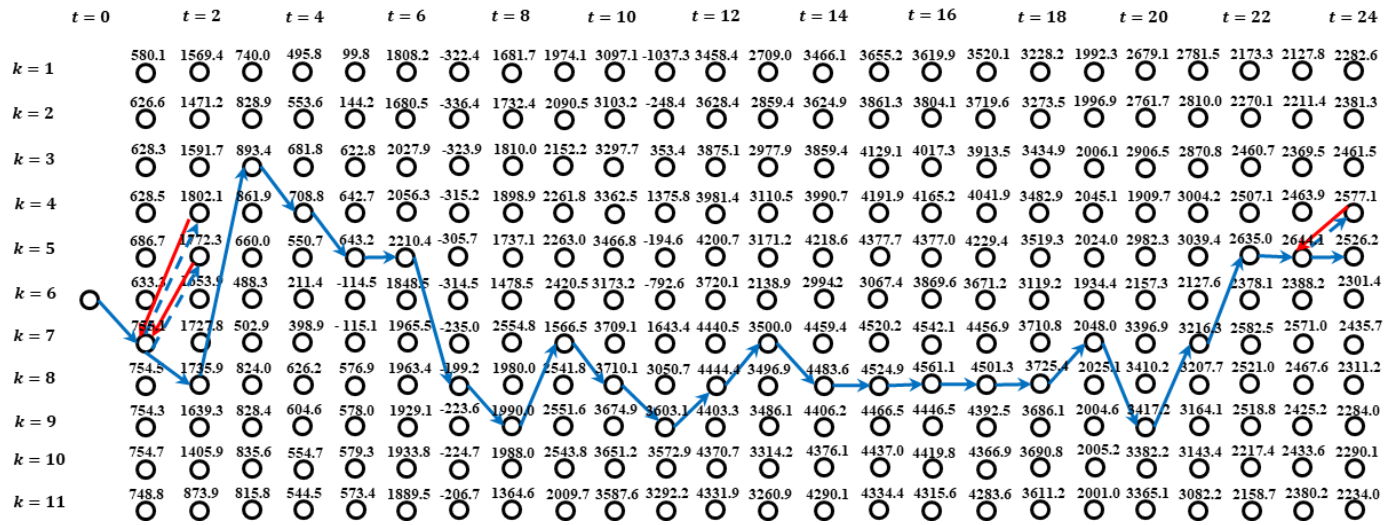

Fig. 6. The most profitable and feasible path obtained by the proposed FBDP.

TABLE II
THE PROFITS OF THE MOST PROFITABLE PARETO SOLUTIONS OF RISK SEEKER/NEUTRAL/AVERSE MH-IGDT MODELS AND THE PROFIT OF THE PROPOSED FBDP

$k=1$	$k=2$	$k=3$	$k=4$	$k=5$	$k=6$	$k=7$	$k=8$	$k=9$	$k=10$	$k=11$	Proposed
48,380.0	50,848.9	55,017.5	56,755.9	57,434.8	46,553.5	60,354.2	63,244.7	63,030.8	62,042.8	59,142.2	64,833.1

TABLE III
THE VPP PROFITS AND OBTAINED BY DIFFERENT MOMP METHODS

Method	WS	NBI	NNC	MAEC	ANNC	ENNC (proposed)
Profit ($)	52,448.5	58,989.3	60,242.3	62,351.5	62,742.6	64,833.1

TABLE IV
COMPARISON OF THE PROPOSED APPROACH WITH SP METHODS

Method	SP1	SP2	SP3	Proposed
Profit ($)	52,420.2	52,779.3	53,022.9	59,500.1
Exe. time (min)	3:23	7:09	13:31	7:58

TABLE V
COMPARISON OF THE PROPOSED APPROACH WITH FOSD METHODS

Method	FOSD1	FOSD2	FOSD3	Proposed
Profit ($)	53,279.5	53,414.6	53,513.6	59,500.1
Exe. time (min)	14:19	14:53	15:37	7:58

TABLE VI
COMPARISON OF THE PROPOSED APPROACH WITH SOSD METHODS

Method	SOSD1	SOSD2	SOSD3	Proposed
Profit ($)	53,086.5	53,207.1	53,301.8	59,500.1
Exe. time (min)	14:03	14:31	15:18	7:58

TABLE VII
COMPARISON OF THE PROPOSED APPROACH WITH CVAR-BASED SP METHODS

Method	CVaR1	CVaR2	CVaR3	Proposed
Profit ($)	54,298.7	53,566.7	53,333.1	59,500.1
Exe. time (min)	13:42	13:55	14:11	7:58

methods, denoted by FOSD1, FOSD2, and FOSD3, have 20, 50, 100 benchmark scenarios.

- Second-order stochastic dominance (SOSD) with three different numbers of benchmark scenarios in Table VI [33]. These SOSD methods, denoted by SOSD1, SOSD2, and SOSD3, have 20, 50, 100 benchmark scenarios.
- CVaR-based SP with three different confidence intervals in Table VII [5]. These CVaR-based SP methods, denoted by CVaR1, CVaR2, and CVaR3, have 0.9, 0.95, and 0.99 confidence intervals.

These uncertainty modeling approaches have been considered as comparative methods in the Tables IV, V, VI, and VII since these methods have been used for VPP self-scheduling in the previous works, such as in [3], [4], [5], [32] and [33]. As these comparative methods and the proposed approach have different uncertainty modeling strategies, for the sake of a fair comparison, an out-of-sample analysis with the same set of out-of-sample scenarios [21] has been used to evaluate the performance of all methods in Tables IV, V, VI, and VII. For this reason, the result reported for the proposed approach in Table III (which has been obtained using the in-sample scenarios) is different from the result reported in Tables IV-VII (which has been obtained using the out-of-sample scenarios). Table IV shows that by increasing the number of scenarios, the profit of SP methods increases as the uncertainty spectrum can be better captured. The SP3 method of Table IV with 100 scenarios has been used for the comparative methods of Tables V, VI, and VII, which are SP methods with risk measures. The comparative methods in Tables V, VI, and VII have higher profits than the SP methods in Table IV, since the comparative methods in Tables V, VI, and VII incorporate risk measures. FOSD and SOSD comparative methods in Tables V and VI have similar performances. The profit of these methods slightly increases by increasing the number of their benchmark scenarios which are different from the 100 scenarios of SP3. Moreover, it is seen that CVaR-based SP leads to higher profits than other comparative methods in Tables IV, V, and VI, since CVaR is a more coherent risk measure [34].

It is seen that the proposed VPP self-scheduling strategy outperforms all of the 12 comparative methods in Tables IV, V, VI, and VII due to the following reasons: 1) The proposed approach can find both robust solutions using unfavorable deviations of uncertain parameters and opportunistic solutions using favorable deviations of uncertain parameters, 2) The proposed approach can provide both the risk-averse and risk-seeker Pareto frontiers for VPP self-scheduling problem. In addition, it can find the most effective Pareto solution of each Pareto frontier, 3) The proposed approach can adaptively decide to act as either risk-averse or risk-seeker in each hour of the scheduling horizon to maximize the VPP profit, and 4) The proposed approach can adaptively determine optimal risk-averting/seeking level for each scheduling hour. In other words, the proposed approach provides adaptive bi-directional decision-making capability with optimized risk averting/seeking levels. The above features are specific to the proposed VPP self-scheduling strategy.

Tables IV, V, VI, and VII show that only the computation times of SP1 and SP2 are slightly lower than the computation time of the proposed method. However, the computation time of the proposed method is lower than the computation time of all other methods of Tables IV, V, VI, and VII.

C. Evaluating the Impact of the Standard deviations of the Uncertain Parameters

To evaluate the impact of the standard deviations of the uncertain parameters on the proposed VPP self-scheduling approach, these standard deviations are halved/doubled with

TABLE VIII
THE VPP PROFITS OBTAINED FOR CASES I, II, AND III

Case	I	II	III
Profit ($)	67,769.7	64,833.1	59,599.7

TABLE IX
THE MOST PROFITABLE AND FEASIBLE PATH OBTAINED IN CASES I, II, AND III

	$t=1$	$t=2$	$t=3$	$t=4$	$t=5$	$t=6$	$t=7$	$t=8$	$t=9$	$t=10$	$t=11$	$t=12$	$t=13$	$t=14$	$t=15$	$t=16$	$t=17$	$t=18$	$t=19$	$t=20$	$t=21$	$t=22$	$t=23$	$t=24$
Case I	$k=7$	$k=7$	$k=3$	$k=5$	$k=4$	$k=3$	$k=7$	$k=9$	$k=7$	$k=8$	$k=8$	$k=7$	$k=7$	$k=7$	$k=8$	$k=8$	$k=8$	$k=7$	$k=7$	$k=8$	$k=8$	$k=5$	$k=5$	$k=4$
Case II	$k=7$	$k=8$	$k=3$	$k=4$	$k=5$	$k=5$	$k=8$	$k=9$	$k=7$	$k=8$	$k=9$	$k=8$	$k=7$	$k=8$	$k=8$	$k=8$	$k=8$	$k=8$	$k=7$	$k=9$	$k=7$	$k=5$	$k=5$	$k=5$
Case III	$k=7$	$k=8$	$k=5$	$k=5$	$k=5$	$k=8$	$k=7$	$k=9$	$k=6$	$k=9$	$k=10$	$k=9$	$k=8$	$k=9$	$k=7$	$k=9$	$k=9$	$k=9$	$k=7$	$k=7$	$k=7$	$k=9$	$k=8$	$k=8$

TABLE X
RESULTS OF THE PROPOSED VPP SELF-SCHEDULING STRATEGY FOR DIFFERENT NETWORK INJECTION LIMITS

Network Limitation (MW)	110	100	90	80	70	60	50	40	30	20	10	0
Profit ($)	64,833.1	64,833.1	64,184.8	62,343.0	59,045.3	53,960.5	47,059.5	39,506.2	33,085.0	27,631.8	23,059.8	19,235.8

respect to their base values, which are referred to as Case I/III. The base case is referred to as Case II. The profits obtained by the proposed VPP self-scheduling approach for these three cases are shown in Table VIII. It is seen that the VPP profit decreases from Case I to Case III. Its reason is that from Case I to Case III, the standard deviations of the uncertain parameters increase, leading to higher volatility of wind power, load and price, and thus their forecast accuracies decrease. In Table VIII, the most profitable and feasible paths obtained in Cases I-III are shown. The path of Case II is the same path shown in Fig. 6, and it is again illustrated in Table VIII for the sake of comparison with the other cases. Also, only the state selected in each hour is shown in Table IX for the sake of conciseness. By comparing the results of the three cases in Table IX it is seen that:

a) Case I with respect to Case II has more risk-averse state (i.e., with a higher k value) in 1 hour, the same states (i.e., with the same k values) in 12 hours, and more risk-seeker states (i.e., with lower k values) in 11 hours. Thus, overall, Case I becomes more risk-seeker with respect to Case II as more accurate forecasts are used in Case I, which allows adopting a more risk-seeking self-scheduling strategy.

b) Case III with respect to Case II has more risk-seeker states (i.e., with lower k values) in 4 hours, the same states (i.e., with the same k values) in 6 hours, and more risk-averse states (i.e., with higher k values) in 14 hours. Thus, overall, Case III becomes more risk-averse with respect to Case II as less accurate forecasts are used in Case III, which leads to a more risk-averting (or more conservative) decision-making strategy.

D. Evaluating the Impact of Network Injection Limit and Wind Spillage

To model the limit of power injection to/from the grid and wind spillage in the proposed VPP self-scheduling strategy, each of the deterministic model (1), risk-averse MH-IGDT model (8), risk seeker MH-IGDT model (10), and in-sample scenario formulation (13) is changed as follows:

1) Changes applied to the deterministic model. Network constraint $|P_{bt}^{N}| \le P_{bt}^{N,max}$ is explicitly added to the deterministic model (1) as a new constraint (1p). To model wind spillage, wind power variable P_{ut} (which is $\bar{P}_{ut}$ minus wind power spillage) replaces $\bar{P}_{ut}$ in (1b) for wind units $u \in \Omega_{W^b}$. Moreover, the constraint $0 \le P_{ut} \le \bar{P}_{ut}, u \in \Omega_W$ is added as (1q) to the deterministic model.

2) Changes applied to the risk-averse/seeker MH-IGDT models. At first, (1b)-(1o) in (5b) is replaced by (1b)-(1p) to include network injection limit (1p) in the MH-IGDT models. Moreover, to include wind spillage, (7c) is replaced by $0 \le P_{ut} \le (1-\hat{\alpha}_w).\bar{P}_{ut},\ \forall u \in \Omega_W, \forall t$ in the risk-averse MH-IGDT model, and (9c) is replaced by $0 \le P_{ut} \le (1+\check{\alpha}_w).\bar{P}_{ut}$, $\forall u \in \Omega_W, \forall t$ in the risk-seeker MH-IGDT model. Thus, (8) with updated (5b) and (7c), and (10) with updated (6b) and (9c) represent risk-averse/seeker MH-IGDT models, respectively, including network injection limit and wind spillage.

3) Changes applied to the in-sample scenario formulation. The network constraint $\left|P_{bt}^{N,j\zeta}\right| \le P_{bt}^{N,max}$ is added as a new constraint (13s) to in-sample scenario formulation given in (13). To model wind spillage, similar to the changes applied to the deterministic model, the wind power variable $P_{ut}^{j\zeta}$ replaces P_{ut}^{ζ} in (13b) for wind units $u \in \Omega_{W^b}$. Moreover, the constraint $0 \le P_{ut}^{j\zeta} \le P_{ut}^{\zeta}, u \in \Omega_W$ is added as (13t) to (13).

The solution of the proposed VPP self-scheduling strategy including network injection limit and wind power spillage, as described above, is reported in the following Table X for different network injection limit values. In Table X, the network injection limit is decreased from its base value 110MW in 10MW steps to zero. At first, by decreasing the network injection limit from 110MW to 100MW, the VPP profit is not changed, since the 100MW limit is still larger than the maximum capacity that the VPP can inject to the network. However, by further decreasing the network injection limit from 100MW to zero, the VPP profit monotonically decreases from the base value $64,833.1 to $19,235.8. However, it is seen that no infeasibility occurs and only the VPP profit decreases. Its reason is that, for lower network injection limit values, the proposed VPP self-scheduling strategy reduces the generation of dispatchable units and the generation of wind units (using wind spillage) such that the network injection limit is satisfied. Even with the most serious network injection limit (i.e., 0MW limit), the proposed approach decreases the generation of dispatchable and wind units to solely supply the VPP load demand (similar to the operation of an islanded microgrid).

Some risk-seeker solutions with a high UB value may become infeasible due to violation of the constraint (10b). It is possible that a high UB value excessively increases the right-hand side $(1+UB).\bar{\mathcal{F}}$ such that no feasible profit can be obtained. Considering network injection limits may intensify this case, since considering network injection limits may lead to decreasing the VPP generation and thus may decrease the profits of the risk seeker/averse solutions. However, even if some risk-seeker solutions become infeasible, no infeasibility problem occurs for the proposed approach and its solution becomes feasible in all cases as reported in Table X. Its reason is as follows.

The ENNC produces 45 Pareto solutions for each UB value. If one of these solutions becomes infeasible, the ENNC filters it and the best Pareto solution is found among the remaining 44 feasible solutions. Even if, in an extreme case, all 45 Pareto solutions produced for one UB value become infeasible (which is very unlikely), again no infeasibility problem occurs for the proposed VPP self-scheduling approach, since the corresponding state (i.e., the corresponding UB value) is removed from the

TABLE B1
THE DISPATCHABLE UNITS' DATA SET [25]

Unit	SU_u^r, SD_u^r (MW/Min)	RU_u, RD_u (MW/Min)	τ_u^{on}, τ_u^{off} (Hour)	A_u($), B_u($/MW)	SU_u^c, SD_u^c ($)
2×12MW	2, 12	1, 1	2, 4	5.9, 13.6	132.1, 13.2
1×20MW	6, 20	3, 3	0, 0	9.4, 27.1	31.7, 3.2

TABLE B2
THE EXPECTED VALUES OF LMP ($/MWH), WIND SPEED (M/S), AND LOAD (MW) OF THE GENERATED SCENARIOS FOR PERFORMANCE EVALUATION METHOD

	$t=1$	$t=2$	$t=3$	$t=4$	$t=5$	$t=6$	$t=7$	$t=8$	$t=9$	$t=10$	$t=11$	$t=12$	$t=13$	$t=14$	$t=15$	$t=16$	$t=17$	$t=18$	$t=19$	$t=20$	$t=21$	$t=22$	$t=23$	$t=24$
LMP	45.3	44.5	37.2	36.8	38.3	51.1	75.6	71.7	67.3	75.9	79.1	76.6	75.7	77.5	77.1	76.6	77.3	79.4	88.1	97.6	74.7	62.2	60.7	57.2
Wind speed	4.5	8.4	9.0	7.9	6.6	8.3	6.6	4.5	6.6	7.9	9.1	9.2	7.2	9.4	9.2	9.1	9.1	7.2	3.6	4.9	6.9	7.9	8.3	9.1
Load	13.0	12.2	11.7	11.4	11.4	11.7	14.4	16.7	18.5	18.6	18.6	18.4	18.5	18.5	18.0	18.2	19.2	19.4	19.4	18.6	17.7	16.1	14.2	12.2

FBDP and the most profitable path is searched among the remaining states. Thus, no infeasibility occurs for the proposed VPP self-scheduling approach (without or with considering network injection limits) due to its ENNC and FBDP even if some risk-seeker MH-IGDT solutions become infeasible.

VI. CONCLUSION

This paper proposes a new VPP self-scheduling strategy composed of MH-IGDT, ENNC, and bi-directional decision-making approach. To optimize the uncertainty horizons of uncertain parameters such that the predetermined profit is guaranteed, the MH-IGDT is proposed. The ENNC framework, comprising ANNC and lexicographic optimization, is proposed as a new MOMP solution approach to solve the MH-IGDT models. The ANNC part of the proposed ENNC ensures the efficiency and even distribution of Pareto optimal solutions while the lexicographic optimization optimizes the ranges of the uncertainty horizons. Finally, the bi-directional decision maker comprising ex-ante performance evaluation and FBDP is proposed to find the most profitable and feasible path among risk-seeker/neutral/averse states over the scheduling horizon such that the VPP inter-temporal constraints are satisfied. Thus, the two main questions of VPP (i.e., deciding to act as either risk-seeker or risk-averse participant in the market and determining the level of risk-seeking/averting) are adaptively replied for each hour of the scheduling horizon in this paper.

APPENDIX A

For the sake of clarity, the bi-level risk-averse/seeker self-scheduling models (5)/(6) are written as (A1)-(A5)/(A6)-(A10):

$$\underset{\Xi \in \{\pounds(\bar{\Theta}+\Delta\Theta) \cup (A3)\}}{Max} \ (\breve{\alpha}_\lambda, \breve{\alpha}_w, \breve{\alpha}_l) \quad \text{(A1)}$$

where

(5b) (A2)

$$\breve{\mathcal{F}}^*(\bar{\Theta}+\Delta\Theta, \Xi) \geq (1-UB).\bar{\mathcal{F}} \quad \text{(A3)}$$

$$\breve{\mathcal{F}}^*(\bar{\Theta}+\Delta\Theta, \Xi) = \underset{\Delta\Theta}{Min} \ \ \mathcal{F}(\bar{\Theta}+\Delta\Theta, \Xi) \quad \text{(A4)}$$

subject to:

(5d)-(5f) (A5)

$$\underset{\Xi \in \{\pounds(\bar{\Theta}+\Delta\Theta) \cup (A8)\}}{Min} \ (\hat{\alpha}_\lambda, \hat{\alpha}_w, \hat{\alpha}_l) \quad \text{(A6)}$$

where

(5b) (A7)

$$\hat{\mathcal{F}}^*(\bar{\Theta}+\Delta\Theta, \Xi) \geq (1+UB).\bar{\mathcal{F}} \quad \text{(A8)}$$

$$\hat{\mathcal{F}}^*(\bar{\Theta}+\Delta\Theta, \Xi) = \underset{\Delta\Theta}{Max} \ \ \mathcal{F}(\bar{\Theta}+\Delta\Theta, \Xi) \quad \text{(A9)}$$

subject to:

(6d)-(6f) (A10)

where the constraints (5c)/(6c) are replaced by (A3)-(A4)/(A8)-(A9) in the above formulations to better discriminate the upper and lower levels. Based on these formulations, the upper/lower-level problems of the bi-level optimization (5) are (A1)-(A3)/(A4)-(A5) and the upper/lower-level problems of the bi-level optimization (6) are (A6)-(A8)/(A9)-(A10). The objectives of the upper-level problem in (5)/(6) are the uncertainty horizons specified in (A1)/(A6). The constraints of the upper-level problem in (5)/(6) include the solution space constraints (5b) and the admissible profit constraints (A3)/(A8). The decision variables of the upper-level problem in (5)/(6) are:

$$\Xi = \{(I_{ut}, x_{ut}, y_{ut}, P_{ut}), \forall u \in \Omega_D; (I^r_{ut}, I^s_{ut}, P^r_{ut}, P^s_{ut}), \forall u \in \Omega_S\} \quad \forall t \quad \text{(A11)}$$

The objective and constraints of the lower-level problems in (5)/(6) are the VPP profit specified in (A4)/(A9) and the bounded intervals of the uncertain parameters given in (A5)/(A10). The decision variables of the lower-level problems in (5)/(6) are the deviations of the uncertain parameters:

$$\Delta\Theta = \{\Delta\lambda_{bt}, \forall b; \Delta P_{ut}, \forall u \in \Omega_W; \Delta P_{lt}, \forall l\} \quad \forall t \quad \text{(A12)}$$

APPENDIX B

The technical and economic parameters of dispatchable units are given in Table B1. The expected values of LMP, wind speed, and load of the generated scenarios for the ex-ante performance evaluation method are given in Table B2. Also, the standard deviations of LMP, wind speed, and load in the generated scenarios are 0.15, 0.25, and 0.05 of their hourly forecast values. Determination of the balancing prices $\lambda^{\zeta,+}_{bt}/\lambda^{\zeta,-}_{bt}$ depends on the electricity market regulation. For instance, the determination of $\lambda^{\zeta,+}_{bt}/\lambda^{\zeta,-}_{bt}$ in the Iberian Peninsula electricity market and Iran's electricity market has been described in [35] and [36]. As discussed in [35], there should be $\lambda^{\zeta,+}_{bt} \leq \lambda^{\zeta}_{bt}$ and $\lambda^{\zeta,-}_{bt} \geq \lambda^{\zeta}_{bt}$. Here, in the generated scenarios for the ex-ante performance evaluation method, $\lambda^{\zeta,+}_{bt} = 0.5\lambda^{\zeta}_{bt}$ and $\lambda^{\zeta,-}_{bt} = 2\lambda^{\zeta}_{bt}$ are considered.

REFERENCES

[1] D. Pudjianto, C. Ramsay, and G. Strbac, "Virtual power plant and system integration of distributed energy resources," *IET Renew. Power Gener.*, vol. 1, no. 1, p. 10, 2007.

[2] E. Mashhour and S. M. Moghaddas-Tafreshi, "Bidding Strategy of Virtual Power Plant for Participating in Energy and Spinning Reserve Markets—Part I: Problem Formulation," *IEEE Trans. Power Syst.*, vol. 26, no. 2, pp. 949–956, May 2011.

[3] M. A. Tajeddini, A. Rahimi-Kian, and A. Soroudi, "Risk averse optimal operation of a virtual power plant using two stage stochastic programming," *Energy*, vol. 73, pp. 958–967, Aug. 2014.

[4] P. Karimyan, M. Abedi, S. H. Hosseinian, R. Khatami, and M. Abedi, "Stochastic approach to represent distributed energy resources in the form of a virtual power plant in energy and reserve markets," *IET Gener. Transm. Distrib.*, vol. 10, no. 8, pp. 1792–1804, May 2016.

[5] S. R. Dabbagh and M. K. Sheikh-El-Eslami, "Risk Assessment of Virtual Power Plants Offering in Energy and Reserve Markets," *IEEE Trans. Power Syst.*, vol. 31, no. 5, pp. 3572–3582, Sep. 2016.

[6] M. Peik-Herfeh, H. Seifi, and M. K. Sheikh-El-Eslami, "Decision

making of a virtual power plant under uncertainties for bidding in a day-ahead market using point estimate method," *Int. J. Electr. Power Energy Syst.*, vol. 44, no. 1, pp. 88–98, Jan. 2013.

[7] Q. Zhao, Y. Shen, and M. Li, "Control and Bidding Strategy for Virtual Power Plants With Renewable Generation and Inelastic Demand in Electricity Markets," *IEEE Trans. Sustain. Energy*, vol. 7, no. 2, pp. 562–575, Apr. 2016.

[8] L. Wu, M. Shahidehpour, and Z. Li, "Comparison of Scenario-Based and Interval Optimization Approaches to Stochastic SCUC," *IEEE Trans. Power Syst.*, vol. 27, no. 2, pp. 913–921, May 2012.

[9] M. Rahimiyan and L. Baringo, "Strategic Bidding for a Virtual Power Plant in the Day-Ahead and Real-Time Markets: A Price-Taker Robust Optimization Approach," *IEEE Trans. Power Syst.*, vol. 31, no. 4, pp. 2676–2687, Jul. 2016.

[10] M. Shabanzadeh, M.-K. Sheikh-El-Eslami, and M.-R. Haghifam, "The design of a risk-hedging tool for virtual power plants via robust optimization approach," *Appl. Energy*, vol. 155, pp. 766–777, Oct. 2015.

[11] M. Vahid-Ghavidel, N. Mahmoudi, and B. Mohammadi-Ivatloo, "Self-Scheduling of Demand Response Aggregators in Short-Term Markets Based on Information Gap Decision Theory," *IEEE Trans. Smart Grid*, vol. 10, no. 2, pp. 2115–2126, Mar. 2019.

[12] S. Shafiee, H. Zareipour, A. M. Knight, N. Amjady, and B. Mohammadi-Ivatloo, "Risk-Constrained Bidding and Offering Strategy for a Merchant Compressed Air Energy Storage Plant," *IEEE Trans. Power Syst.*, pp. 1–1, 2016.

[13] Y. Ben-Haim, *Info-Gap Decision Theory: Decisions under Severe Uncertainty*, 2nd ed. San Diego, CA: Academic Press, 2006.

[14] S. Dehghan, A. Kazemi, and N. Amjady, "Multi-objective robust transmission expansion planning using information-gap decision theory and augmented ε-constraint method," *IET Gener. Transm. Distrib.*, vol. 8, no. 5, pp. 828–840, 2014.

[15] A. Attarha and N. Amjady, "Solution of security constrained optimal power flow for large-scale power systems by convex transformation techniques and Taylor series," *IET Gener. Transm. Distrib.*, vol. 10, no. 4, pp. 889–896, Mar. 2016.

[16] A. Messac, A. Ismail-Yahaya, and C. A. Mattson, "The normalized normal constraint method for generating the Pareto frontier," *Struct. Multidiscip. Optim.*, vol. 25, no. 2, pp. 86–98, 2003.

[17] B. Bagheri and N. Amjady, "Stochastic multiobjective generation maintenance scheduling using augmented normalized normal constraint method and stochastic decision maker," *Int. Trans. Electr. Energy Syst.*, vol. 29, no. 2, p. e2722, Feb. 2019.

[18] G. Mavrotas, "Effective implementation of the ε-constraint method in Multi-Objective Mathematical Programming problems," *Appl. Math. Comput.*, vol. 213, no. 2, pp. 455–465, Jul. 2009.

[19] X. Gu and H. Zhong, "Optimisation of network reconfiguration based on a two-layer unit-restarting framework for power system restoration," *IET Gener. Transm. Distrib.*, vol. 6, no. 7, p. 693, 2012.

[20] J. Aghaei, N. Amjady, and H. A. Shayanfar, "Multi-objective electricity market clearing considering dynamic security by lexicographic optimization and augmented epsilon constraint method," *Appl. Soft Comput. J.*, vol. 11, no. 4, pp. 3846–3858, 2011.

[21] M. Yazdaninejad and N. Amjady, "Risk-minimizing stochastic self-scheduling model for microgrid in day-ahead electricity market," *Int. Trans. Electr. Energy Syst.*, vol. 27, no. 5, p. e2302, May 2017.

[22] S. A. Hosseini, N. Amjady, M. Shafie-khah, and J. P. S. Catalão, "A new multi-objective solution approach to solve transmission congestion management problem of energy markets," *Appl. Energy*, vol. 165, pp. 462–471, Mar. 2016.

[23] M. Derafshian, N. Amjady, and S. Dehghan, "Special protection scheme against voltage collapse," *IET Gener. Transm. Distrib.*, vol. 10, no. 2, pp. 341–351, Feb. 2016.

[24] A. J. Wood, B. F. Wollenberg, and G. B. Sheblé, *Power Generation, Operation, and Control*, 3rd ed. New York, NY, USA: Wiley-Intersience, 2013.

[25] C. Grigg *et al.*, "The IEEE Reliability Test System-1996. A report prepared by the Reliability Test System Task Force of the Application of Probability Methods Subcommittee," *IEEE Trans. Power Syst.*, vol. 14, no. 3, pp. 1010–1020, 1999.

[26] "Milwood weather forecast." [Online]. Available: http://www.wunderground.com/history/airport/KHPN/.

[27] NYISO, "Actual load, integrated real-time & Pricing data, zonal day-ahead market LBMP." [Online]. Available: http://www.nyiso.com.

[28] GAMS, "The Solver Manuals," 1996. [Online]. Available: http://www.gams.com.

[29] R. T. Marler and J. S. Arora, "The weighted sum method for multi-objective optimization: new insights," *Struct. Multidiscip. Optim.*, vol. 41, no. 6, pp. 853–862, Jun. 2010.

[30] I. Das and J. E. Dennis, "Normal-Boundary Intersection: A New Method for Generating the Pareto Surface in Nonlinear Multicriteria Optimization Problems," *SIAM J. Optim.*, vol. 8, no. 3, pp. 631–657, Aug. 1998.

[31] M. Esmaili, N. Amjady, and H. A. Shayanfar, "Multi-objective congestion management by modified augmented ε-constraint method," *Appl. Energy*, vol. 88, no. 3, pp. 755–766, Mar. 2011.

[32] M. Shabanzadeh, M.-K. Sheikh-El-Eslami, and M.-R. Haghifam, "Risk-based medium-term trading strategy for a virtual power plant with first-order stochastic dominance constraints," *IET Gener. Transm. Distrib.*, vol. 11, no. 2, pp. 520–529, Jan. 2017.

[33] M. Shabanzadeh, M.-K. Sheikh-El-Eslami, and M.-R. Haghifam, "An interactive cooperation model for neighboring virtual power plants," *Appl. Energy*, vol. 200, pp. 273–289, Aug. 2017.

[34] A. J. Conejo, M. Carrión, and J. M. Morales, *Decision Making Under Uncertainty in Electricity Markets*. Boston, MA: Springer US, 2010.

[35] J. M. Morales, A. J. Conejo, and J. Perez-Ruiz, "Short-Term Trading for a Wind Power Producer," *IEEE Trans. Power Syst.*, vol. 25, no. 1, pp. 554–564, Feb. 2010.

[36] N. Amjady, A. A. Rashidi, and H. Zareipour, "Stochastic security-constrained joint market clearing for energy and reserves auctions considering uncertainties of wind power producers and unreliable equipment," *Int. Trans. Electr. Energy Syst.*, vol. 23, no. 4, pp. 451–472, May 2013.